ISSN 0036-0236, Russian Journal of Inorganic Chemistry, 2018, Vol. 63, No. 9, pp. 1225–1231. © Pleiades Publishing, Ltd., 2018.
Original Russian Text © A.V. Ruseikina, L.A. Solov'ev, E.O. Galenko, M.V. Grigor'ev, 2018, published in Zhurnal Neorganicheskoi Khimii, 2018, Vol. 63, No. 9, pp. 1204–1211.

PHYSICAL METHODS OF INVESTIGATION

Refined Crystal Structures of $SrLnCuS_3$ (Ln = Er, Yb)

A. V. Ruseikina[a, *], **L. A. Solov'ev**[b], **E. O. Galenko**[a], **and M. V. Grigor'ev**[a]

[a] *University of Tyumen, Tyumen, 625049 Russia*
[b] *Institute of Chemistry and Chemical Technology, Russian Academy of Sciences, Siberian Branch, Federal Research Center "Krasnoyarsk Scientific Center SB RAS", Krasnoyarsk, 660049 Russia*
**e-mail: adeschina@mail.ru*

Received May 12, 2017

Abstract—According to powder X-ray diffraction data, the crystal structures of compounds $SrLnCuS_3$ (Ln = Er, Yb) have been refined by minimizing the derivative difference in the anisotropic approximation for all atoms. Crystals are orthorhombic, space group *Cmcm*, structure type $KZrCuS_3$: a = 3.93128(3) Å, b = 12.9709(1) Å, c = 10.1161(1) Å, V = 515.843(9) Å^3, ρ_{calc} = 5.337 g/cm^3, Z = 4, R_{DDM} = 3.73%, R_F = 2.06% ($SrErCuS_3$); a = 3.91448(4) Å, b = 12.9554(1) Å, c = 10.0332(1) Å, V = 508.842(8) Å^3, ρ_{calc} = 5.487 g/cm^3, Z = 4, R_{DDM} = 3.56%, R_F = 1.48% ($SrYbCuS_3$). The structure of $SrLnCuS_3$ is described by [$LnCuS_3$] two-dimensional layers formed by distorted CuS_4 tetrahedra and LnS_6 octahedra with Sr^{2+} ions residing between the layers. The compounds are transparent for IR radiation in the range 3200–1800 cm^{-1}.

DOI: 10.1134/S0036023618090140

Compounds $ALnCuS_3$ (A = Eu, Pb; Ln = Er, Yb) are crystallized in orthorhombic crystal system, space group *Cmcm*, isostructural to $KZrCuS_3$, unit cell parameters: a = 3.8965(1), b = 12.8451(3), c = 10.0028(2) Å ($EuYbCuS_3$); a = 3.911(1), b = 12.956(3), c = 10.064(3) Å ($PbYbCuS_3$); a = 3.916(1), b = 12.934(3), c = 10.106(2) Å ($PbErCuS_3$) [1–6]. In $EuYbCuS_3$ ferromagnetic ordering of Eu^{2+} and Yb^{3+} moments occurs at 5.5 K [1]. The compound is thermally stable up to 1745 ± 4 K and has the following high-temperature polymorphic transitions: α–$EuYbCuS_3$ structure type (ST) $KZrCuS_3$ $\xleftrightarrow{1513\pm4\text{K}}$ β–$EuYbCuS_3$ $\xleftrightarrow{1564\pm4\text{K}}$ γ–$EuYbCuS_3$ $\xleftrightarrow{1594\pm3\text{K}}$ δ–$EuYbCuS_3$ [7]. The proximity of the values of $r_{Eu^{2+}}$1.17 and $r_{Sr^{2+}}$1.18 Å (CN = 6) [8] makes it possible to predict compounds $SrLnCuS_3$ (Ln = Er, Yb) to be formed. The temperatures and enthalpies of high-temperature phase transitions of sulfides $SrLnCuS_3$ were determined: $T_{\alpha\leftrightarrow\beta}$ = 1567 K, $T_{\beta\leftrightarrow\gamma}$ = 1608 K, $T_{\gamma\leftrightarrow\delta}$ = 1621 K ($SrYbCuS_3$); $T_{\alpha\leftrightarrow\beta}$ = 1559 K, $T_{\beta\leftrightarrow\gamma}$ = 1608 K, $T_{\gamma\leftrightarrow\delta}$ = 1621 K ($SrErCuS_3$) [9]. The regularities of the alteration of the mentioned characteristics in $SrLnCuS_3$ (Ln = La–Lu) are determined to be similar to those observed for compounds $EuLnCuS_3$ [1, 10]. When decreasing the Ln^{3+} ionic radius, ST of $SrLnCuS_3$ compounds varies subsequently (annealing at 970 K): ST $BaLaCuS_3$ (Ln = La, Ce, Pr) → ST Eu_2CuS_3 (Ln = Sm, Gd, Ho) → ST $KZrCuS_3$ (Ln = Er, Lu) [7]. In the temperature range 970–1170 K, polymorphic transitions were found for $SrLnCuS_3$ (Ln = La, Ce) [11, 12]. At 1170 K in the series $SrLnCuS_3$ (Ln = La–Lu), four types of crystal structures with orthorhombic crystal system were found: ST Ba_2MnS_3 (Ln = La, Ce) → ST $BaLaCuS_3$ (Ln = Pr, Nd) → ST Eu_2CuS_3 (Ln = Sm, Gd, Tb, Dy, Ho) → ST $KZrCuS_3$ (Ln = Lu) [9]. As far as we know, there are no data available in the literature on the determination of the crystal structures and refinement of the crystallographic parameters of compounds $SrLnCuS_3$ (Ln = Er–Yb, annealing at 1170 K).

The aim of this work is to determine the crystal structures of compounds $SrErCuS_3$ and $SrYbCuS_3$ annealed at 1170 K by powder X-ray diffraction.

EXPERIMENTAL

Cu_2S was prepared from the constituent elements (copper of high purity grade 11-4 and sulfur of high purity grade 15-3, Russian State Standards) in an evacuated and sealed-off quartz ampoule [7, 13, 14]. SrS was prepared when H_2 and H_2S were allowed to react with $SrSO_4$ of chemically pure grade [7, 15, 16]. Hydrogen with a rate of 7–8 L/h was first allowed to pass through a layer of strontium sulfate with increasing the temperature 870 K → 970 K → 1070 K and allowing it to stand at each temperature for 5 h followed by the H_2S stream treatment at 1270 K for 5 h [7].

Table 1. Coordinates of atoms and equivalent thermal parameters in the structures of $SrLnCuS_3$ (Ln = Er, Yb)

Atom	x	y	z	U_{eq}, Å^2
		$SrYbCuS_3$		
Yb	0	0	0	0.0121 (12)
Sr	0	0.74736 (10)	0.25	0.0153 (13)
Cu	0	0.47067 (15)	0.25	0.0179 (17)
S(1)	0	0.36505 (19)	0.0640 (2)	0.014 (2)
S(2)	0	0.0767 (3)	0.25	0.007 (2)
		$SrErCuS_3$		
Er	0	0	0	0.0130 (12)
Sr	0	0.74734 (11)	0.25	0.0201 (13)
Cu	0	0.47136 (16)	0.25	0.0176 (17)
S(1)	0	0.3629 (2)	0.0657 (2)	0.016 (2)
S(2)	0	0.0759 (3)	0.25	0.008 (2)

Sulfides Yb_2S_3 and Er_2S_3 were prepared by an indirect method from oxides of IbO-M and ErO-G grades in a flow of H_2S and CS_2 at 1300 K for 20 h [7, 17, 18]. The sulfides obtained had stoichiometric compositions within the error of chemical analysis. Compounds $SrLnCuS_3$ were prepared by alloying the constituent sulfides taken in stoichiometric amount in the ratio 2SrS : Ln_2S_3 : $1Cu_2S$ in a graphite crucible which was enclosed in an evacuated and sealed-off quartz ampoule. The ampoule was heated in an electrical furnace to 1570 K and then exposed for 30 min. Cooling was performed in the switched-off furnace. Weight portions of the sample were annealed at 1170 K for 1 month [5].

X-ray powder diffraction studies were carried out on a PANalytical X'Pert PRO diffractometer equipped with a PIXcel detector and a graphite monochromator (CuK_α radiation) in the diffraction angle range $12° \leq 2\theta \leq 145°$. Samples were prepared by trituration using an agate mortar. Phases in samples 2SrS : $1Ln_2S_3$: $1Cu_2S$ (Ln = Er, Yb) were identified using the ICDDPDF4 + 2012 database. Unit cell parameters were determined using the ITO software [19]. An analysis of systematic absences showed that $SrLnCuS_3$ (Ln = Er, Yb) had space group *Cmcm* (hkl: $h + k = 2n$; $0kl$: $k = 2n$; $h0l$: $h, l = 2n$; $h00$: $h = 2n$; $0k0$: $k = 2n$; $00l$: $l = 2n$). The initial structure model consisted of the data set for isostructural compound $KZrCuS_3$ [20]. The crystal structures of $SrLnCuS_3$ (Ln = Er, Yb) were refined using the derivative difference minimization (DDM) method [21] in the anisotropic approximation for all atoms, with account for the preferred orientation, anisotropic peak broadening, and surface roughness and displacement of test samples; the final reliability factors were R_{DDM} = 3.56–3.73% and R_F = 1.48–2.06%. In addition to the main phase, the following identified impurities were added to the model to be refined: 1.2% SrS, 2.2% Yb_2SO_2, 1.8% $Yb_5S(SiO_4)_3$ for sample 2SrS : $1Yb_2S_3$: $1Cu_2S$ and 1.2% SrS, 9.5% Er_2SO_2, 0.5% $Er_5S(SiO_4)_3$ for sample 2SrS : $1Er_2S_3$: $1Cu_2S$. Atomic coordinates, equivalent anisotropic thermal parameters, and selected interatomic distances in the structures of $SrLnCuS_3$ are listed in Tables 1–3. Measured, simulated, and difference X-ray diffraction patterns after refinement are shown in Fig. 1. The Diamond 3 program package [22] was used to visualize crystal structures.

IR spectra were recorded in the range 4000–400 cm^{-1} on an FSM 1201 FTIR spectrometer. Samples of $SrLnCuS_3$ were blended with KBr powder to a homogeneous mass with an agate mortar, and pellets were formed [23]. The resulting mixture was placed to a PF-13 die and were pressed using a PRG-400 hydraulic press with a pressure of 213 bar.

Table 2. Anisotropic thermal parameters (Å^2) in the structures of $SrLnCuS_3$ (Ln = Er, Yb)

Atom	U^{11}	U^{22}	U^{33}	U^{12}	U^{13}	U^{23}
			$SrYbCuS_3$			
Yb	0.0108 (15)	0.0120 (14)	0.0136 (14)	0.0000	0.0000	−0.0020 (4)
Sr	0.0070 (15)	0.0097 (15)	0.0291 (18)	0.0000	0.0000	0.0000
Cu	0.0209 (19)	0.017 (2)	0.0156 (19)	0.0000	0.0000	0.0000
S(1)	0.013 (2)	0.010 (2)	0.0204 (19)	0.0000	0.0000	−0.0064 (14)
S(2)	0.012 (3)	0.005 (2)	0.0051 (19)	0.0000	0.0000	0.0000
			$SrErCuS_3$			
Er	0.0134 (11)	0.0108 (10)	0.0149 (9)	0.0000	0.0000	−0.0062 (6)
Sr	0.0150 (14)	0.0107 (12)	0.0346 (13)	0.0000	0.0000	0.0000
Cu	0.0234 (18)	0.0119 (19)	0.0175 (18)	0.0000	0.0000	0.0000
S(1)	0.0165 (17)	0.0133 (19)	0.0172 (18)	0.0000	0.0000	−0.0034 (14)
S(2)	0.012 (3)	0.006 (3)	0.006 (2)	0.0000	0.0000	0.0000

Table 3. Interatomic distances (*d*) in the structures of $SrLnCuS_3$ (Ln = Er, Yb)

Bond	*d*, Å	Bond	*d*, Å	Bond	*d*, Å
		$SrYbCuS_3$			
Yb–S(1)^{i}	4 × 2.702 (2)	Sr–S(1)^{ii}	4 × 3.105 (2)	Cu–S(1)	2 × 2.314 (3)
Yb–S(2)	2 × 2.698 (1)	Sr–S(2)^{ii}	2 × 2.953 (3)	Cu–S(2)^{ii}	2 × 2.391 (2)
⟨Yb–S⟩	**2.701(2)**	**⟨Sr–S⟩**	**3.054(2)**	**⟨Cu–S⟩**	**2.353(2)**
		$SrErCuS_3$			
Er–S(1)^{i}	4 × 2.733 (2)	Sr–S(1)^{ii}	4 × 3.096 (2)	Cu–S(1)	2 × 2.336 (3)
Er–S(2)	2 × 2.714 (1)	Sr–S(2)^{ii}	2 × 2.968 (3)	Cu–S(2)^{ii}	2 × 2.388 (2)
⟨Er–S⟩	**2.727(2)**	**⟨Sr–S⟩**	**3.053(2)**	**⟨Cu–S⟩**	**2.362(2)**

The average values are shown in bold type. Symmetry transformations used to generate equivalent atoms: (i) $x - 1/2, y - 1/2, z$; (ii) $x - 1/2, y + 1/2, z$.

RESULTS AND DISCUSSION

The X-ray powder diffraction patterns of the compounds were indexed in terms of the orthorhombic crystal system, space group *Cmcm* ($KZrCuS_3$ structure type) with the unit cell parameters: $a = 3.93128(3)$ Å, $b = 12.9709(1)$ Å, $c = 10.1161(1)$ Å, $V = 515.843(9)$ Å^3, $\rho_{calc} = 5.337$ g/cm^3, $R_{DDM} = 3.73\%$, $R_F = 2.06\%$ ($SrErCuS_3$), $a = 3.91448(4)$, $b = 12.9554(1)$, $c = 10.0332(1)$ Å, $\rho_{calc} = 5.487$ g/cm^3, $V = 508.842(8)$ Å^3, $R_{DDM} = 3.56\%$, $R_F = 1.48\%$ ($SrYbCuS_3$).

The crystal structure of compounds is of the layer–block type (Fig. 2). Ions Sr^{2+}, Ln^{3+} (Ln = Er, Yb), and Cu^+ occupy independent crystallographic positions. Distorted tetrahedra CuS_4 connected by the vertex atoms S(2) form continuous chains along the *a* axis. Distorted tetrahedra are built of 2 × S(1) + 2 × S(2) atoms. The average bond lengths $d_{Cu-S} = 2.362$ Å in $SrErCuS_3$ (Table 3) is lower than the theoretical value $d_{Cu-S\ (theor)} = 2.44$ Å calculated from the ionic radii $r_{Cu^+} = 0.6$ Å and $r_{S^{2-}} = 1.84$ Å [8]. In distorted tetrahedra of $SrYbCuS_3$, the average Cu–S distance is even shorter being 2.353 Å. Distorted octahedra LnS_6 are in between CuS_4 distorted tetrahedra chains. The octahedral environment of Ln^{3+} is built of four equatorial atoms S1 and two axial atoms S(2) (Fig. 3). The average distances d_{Ln-S} practically coincide with the theoretical values, $d_{Er-S} = 2.727$ Å as compared to $d_{Er-S\ (theor)} = 2.73$ Å ($r_{Er^{3+}} = 0.89$ Å, CN = 6) and $d_{Yb-S} = 2.701$ Å as compared to $d_{Yb-S(theor)} = 2.708$ Å ($r_{Yb^{3+}} = 0.868$ Å, CN = 6), and decrease systematically with decreasing $r_{Ln^{3+}}$ [8]. Distorted octahedra LnS_6, joining the 2 × S(1)S(1) edges along the *a* axis and the 2 × S(2) vertices along the *c* axis, form two-dimensional grids in the *a*–*c* plane. Distorted octahedra LnS_6 and distorted tetrahedra CuS_4 joining 4 × S(1)S(2) edges form parallel $[LnCuS_3]$ layer-blocks perpendicular to the *b* axis. The trigonal prisms SrS_6 are formed by 4 × S(1) and 2 × S(2) atoms with an average d_{Sr-S} distance of 3.053 Å (for $SrErCuS_3$) and 3.054 Å (for $SrYbCuS_3$) whereas $d_{Sr-S\ (theor)} = 3.02$ Å. Trigonal prisms are connected by faces 2 × S(1)S(1)S(2) to form chains along the *a* axis.

The structure of $SrLnCuS_3$ can be described by two-dimensional layers $[LnCuS_3]$ in the *a*–*c* plane formed by distorted tetrahedra CuS_4 and distorted octahedra LnS_6 with Sr^{2+} ions in between.

The determined values of the X-ray diffraction and structural parameters for $SrLnCuS_3$ (Ln = Er, Yb) agree with the regular alteration of the average values of d_{Ln-S} and d_{Cu-S}, unit cell parameters, unit cell volume, and the density calculated based on the X-ray diffraction studies for the series of $SrLnCuS_3$ [7] and correlate with changing $r_{Ln^{3+}}$. Thus, it was found that in $SrLnCuS_3$ (Ln = Gd, Er, Yb, Lu) the values of $a_{Pnma}(c_{Cmcm})$ and $b_{Pnma}(a_{Cmcm})$, d_{Ln-S} and d_{Cu-S} decrease:

$a_{Pnma}(c_{Cmcm})$ = 10.3288(2) ($SrGdCuS_3$ [7]) → 10.1161(1) ($SrErCuS_3$) → 10.0332(1) ($SrYbCuS_3$) → 10.0206(1) ($SrLuCuS_3$ [7]) Å.

$b_{Pnma}(a_{Cmcm})$ = 3.96271(7) ($SrGdCuS_3$ [7]) → 3.93128(3) ($SrErCuS_3$) → 3.91448(4) ($SrYbCuS_3$) → 3.91105(4) ($SrLuCuS_3$ [7]) Å.

d_{Ln-S}: 2.769 (d_{Gd-S} [7]) → 2.727 (d_{Er-S}) → 2.701 (d_{Yb-S}) → 2.699 (d_{Lu-S} [7]) Å;

d_{Cu-S}: 2.366 [7] → 2.362 → 2.353 → 2.350 [7] Å, respectively.

This correlates with changes in the parameters of isomorphous compounds $BaLnMQ_3$ [24] and $EuLnCuS_3$ [10].

Thus, decreased Ln^{3+}radiilead to crystal-chemical compression of the $[LnCuS_3]$ two-dimensional block, which manifests itself in decreased crystallographic (unit cell parameters and unit cell volume) and structural (Cu–S distances and distances between the chains) parameters.

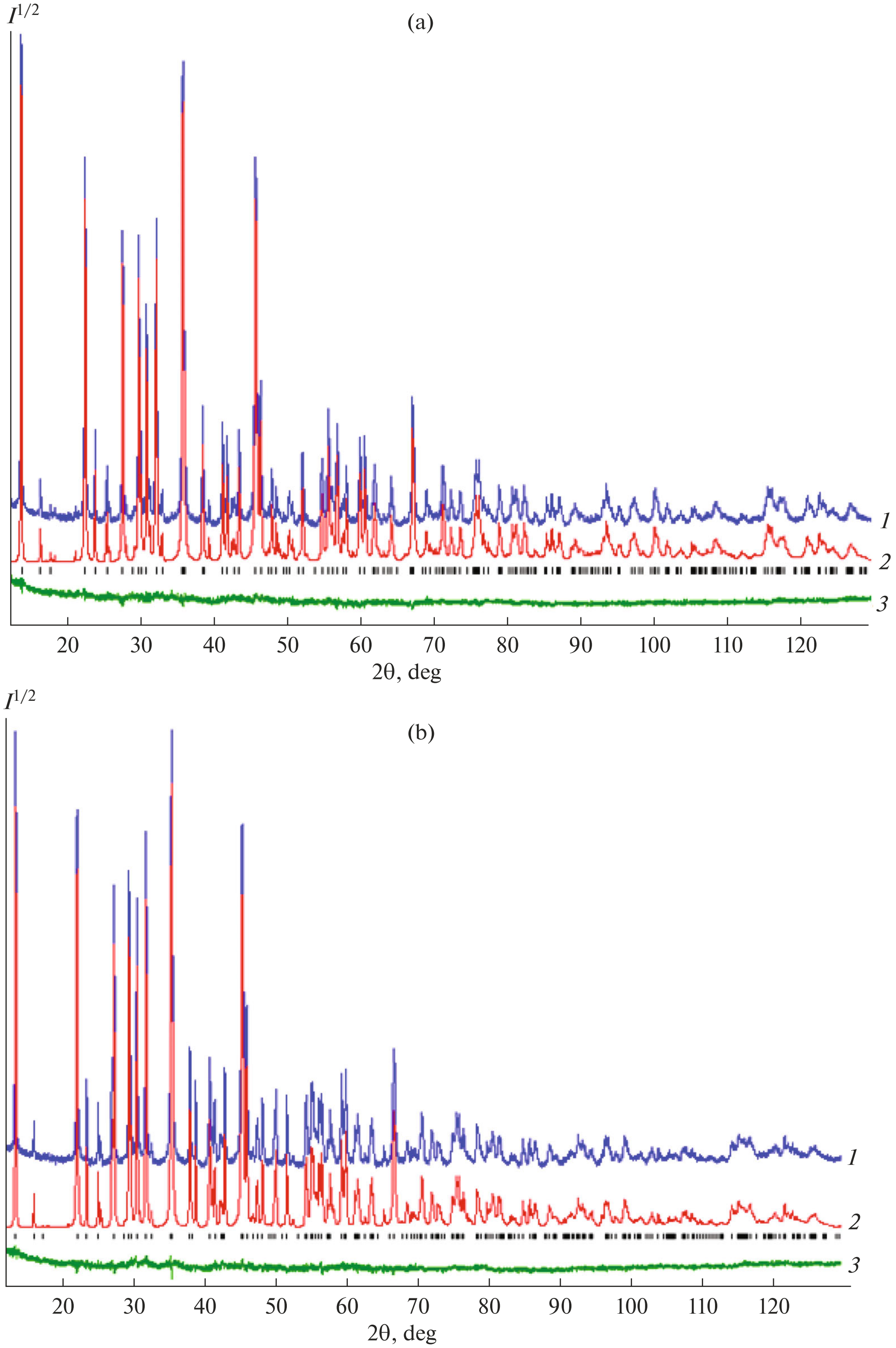

Fig. 1. (1) Measured, (2) simulated, and (3) difference X-ray diffraction patterns of samples (a) 2SrS : $1Yb_2S_3$: $1Cu_2S$ and (b) 2SrS : $1Er_2S_3$: $1Cu_2S$ after the structure has been refined by minimizing the derivative difference. The positions of the main phase peaks are shown in dashes.

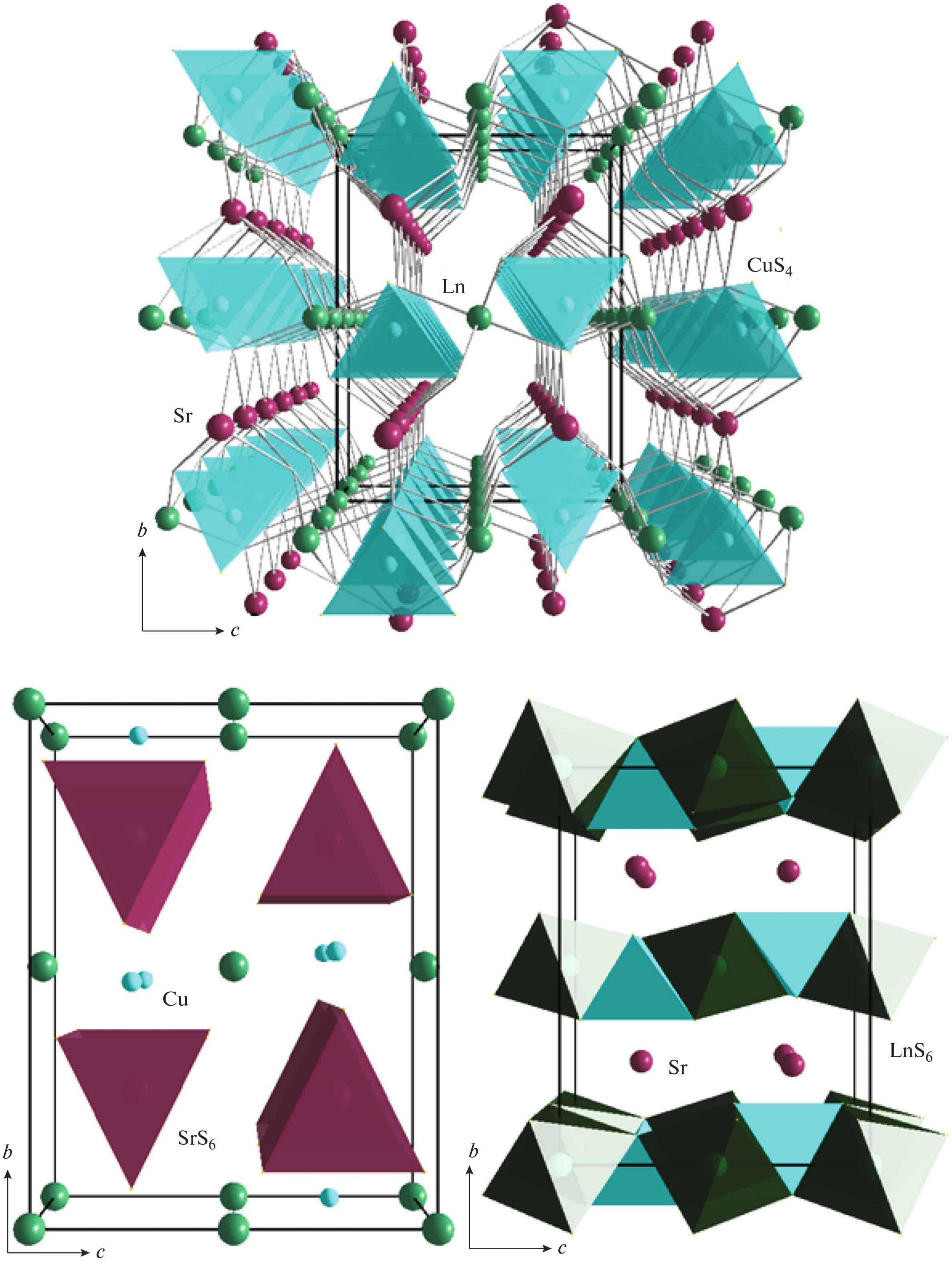

Fig. 2. The [100] projections of the structure of $SrLnCuS_3$.

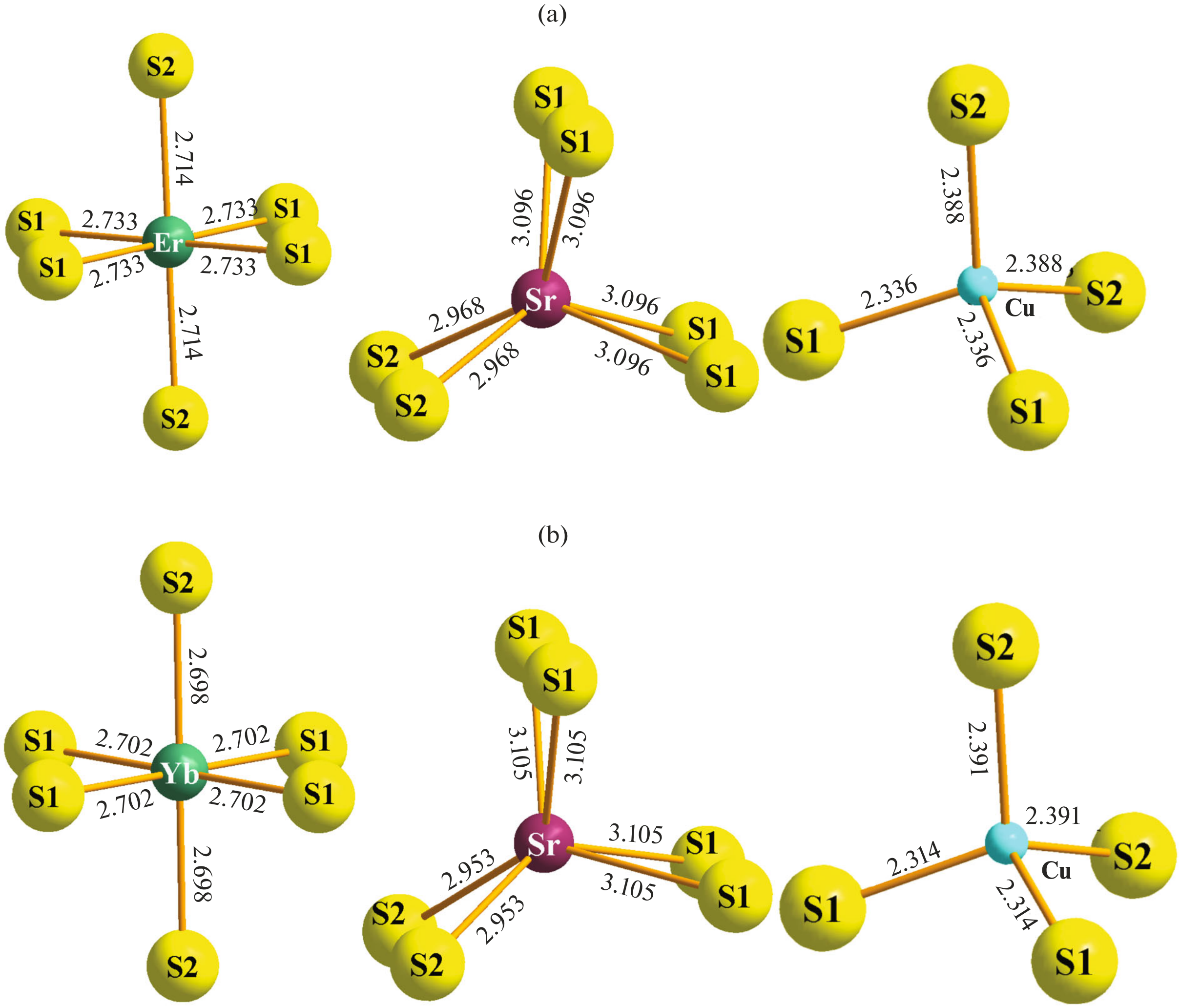

Fig. 3. Coordination environment of Ln, Sr, and Cu in compounds (a) $SrErCuS_3$ and (b) $SrYbCuS_3$.

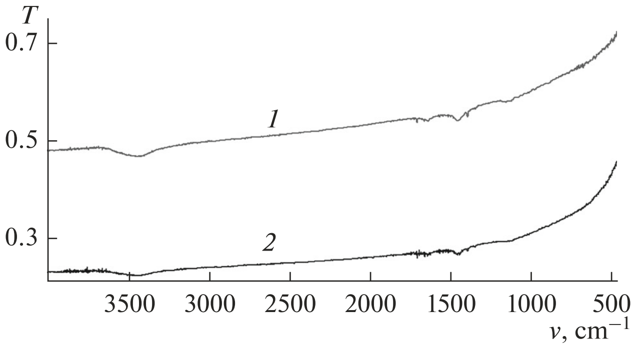

Fig. 4. IR spectra of (*1*) $SrYbCuS_3$ and (*2*) $SrErCuS_3$.

The IR spectra of $SrLnCuS_3$ (Ln = Er, Yb) are shown in Fig. 4. There are no absorption bands in the 3200–1800 cm^{-1} region; the samples are transparent for IR radiation. In the ranges 3600–3300 and 1700–1300 cm^{-1}, the bands of OH-groups vibrations of sorbed water are observed. The presence of trace amounts of water is due to the water sensitivity of sulfides. The annealed surface of sulfides, when exposed to the atmosphere, is particularly capable of adsorbing water during the preparation of pellets. The presence of a spectral background in samples of $SrLnCuS_3$ (Ln = Er, Yb) is determined by the dispersity of the pellet starting material.

Table 4. Selected bond angles (ω) in the structures of $SrLnCuS_3$ (Ln = Er, Yb)

Angle	ω, deg	Angle	ω, deg
		$SrYbCuS_3$	
S(1)$^{\mathrm{i}}$YbS(1)$^{\mathrm{iii}}$	92.84 (7)	S(1)$^{\mathrm{ii}}$SrS(2)$^{\mathrm{ii}}$	87.13 (5)
S(1)$^{\mathrm{i}}$YbS(1)$^{\mathrm{iv}}$	87.16 (7)	S(1)$^{\mathrm{ii}}$SrS(2)$^{\mathrm{vi}}$	141.78 (5)
S(1)$^{\mathrm{i}}$YbS(2)	90.99 (7)	S(2)$^{\mathrm{ii}}$SrS(2)$^{\mathrm{vi}}$	83.03 (10)
S(1)$^{\mathrm{i}}$YbS(2)$^{\mathrm{v}}$	89.01 (7)	S(1)CuS(1)$^{\mathrm{ix}}$	107.50 (14)
S(1)$^{\mathrm{ii}}$SrS(1)$^{\mathrm{vi}}$	78.17 (6)	S(1)CuS(2)$^{\mathrm{ii}}$	109.86 (5)
S(1)$^{\mathrm{ii}}$SrS(1)$^{\mathrm{vii}}$	73.89 (8)	S(2)$^{\mathrm{ii}}$CuS(2)$^{\mathrm{vi}}$	109.89 (17)
S(1)$^{\mathrm{ii}}$SrS(1)$^{\mathrm{viii}}$	121.17 (9)		
		$SrErCuS_3$	
S(1)$^{\mathrm{i}}$ErS(1)$^{\mathrm{iii}}$	92.00 (9)	S(1)$^{\mathrm{ii}}$SrS(2)$^{\mathrm{ii}}$	86.70 (6)
S(1)$^{\mathrm{i}}$ErS(1)$^{\mathrm{iv}}$	88.00 (9)	S(1)$^{\mathrm{ii}}$SrS(2)$^{\mathrm{vi}}$	141.55 (5)
S(1)$^{\mathrm{i}}$ErS(2)	90.54 (7)	S(2)$^{\mathrm{ii}}$SrS(2)$^{\mathrm{vi}}$	82.93 (10)
S(1)$^{\mathrm{i}}$ErS(2)$^{\mathrm{v}}$	89.46 (7)	S(1)CuS(1)$^{\mathrm{ix}}$	105.94 (16)
S(1)$^{\mathrm{ii}}$SrS(1)$^{\mathrm{vi}}$	78.81 (6)	S(1)CuS(2)$^{\mathrm{ii}}$	109.99 (5)
S(1)$^{\mathrm{ii}}$SrS(1)$^{\mathrm{vii}}$	74.06 (8)	S(2)$^{\mathrm{ii}}$CuS(2)$^{\mathrm{vi}}$	110.82 (17)
S(1)$^{\mathrm{ii}}$SrS(1)$^{\mathrm{viii}}$	122.09 (11)		

Symmetry transformations used to generate equivalent atoms: (i) $x - 1/2, y - 1/2, z$; (ii) $x - 1/2, y + 1/2, z$; (iii) $x + 1/2, y - 1/2, z$; (iv) $x - 1/2, -y + 1/2, -z$; (v) $-x, -y, z - 1/2$; (vi) $x + 1/2, y + 1/2, z$; (vii) $-x - 1/2, y + 1/2, -z + 1/2$; (viii) $-x + 1/2, y + 1/2, -z + 1/2$; (ix) $-x, y, -z + 1/2$.

REFERENCES

1. F. Furuuchi and Y. Hinatsu, J. Phys: Condens. Matter **16**, 1088 (2004). doi 10.1088/0953-8984/16/30/012
2. L. D. Gulay, I. D. Olekseyuk, M. Wolcyrz, et al., J. Alloys Compd. **399**, 1016 (2005). doi 10.1016/j.jallcom.2005.03.036
3. L. A. Koscielski, Z. Anorg. Allg. Chem. **15**, 1002 (2012). doi 10.1002/zaac.201200301
4. A. V. Ruseikina, L. A. Solovyov, M. S. Molokeev, and O. V. Andreev, Russ. J. Inorg. Chem. **57**, 79 (2012). doi 10.1134/S0036023612010172
5. A. V. Ruseikina, L. A. Solov'ev, and O. V. Andreev, Russ. J. Inorg. Chem. **58**, 1231 (2013). doi 10.1134/S0036023613100197
6. Yu. A. Murashko, A. V. Ruseikina, A. A. Kislitsyn, and O.V. Andreev, Inorg. Mater. **51**, 1134 (2015). doi 10.1134/S0020168515120079
7. O. V. Andreev, A. V. Ruseikina, L. A. Solov'ev, et al., *Preparation, Structure, and Physicochemical Characteristics of $ALnBS_3$ (A = Sr, Eu; Ln = La-Lu; B = Cu, Ag) Compounds* (RIO UrO RAN, Yekaterinburg, 2014) [in Russian].
8. R. D. Shannon, Acta Crystallogr., Sect. A **32**, 1107 (1976). doi 10.1107/S0567739476001551
9. A. V. Ruseikina, O. V. Andreev, E. O. Galenko, and S. I. Koltsov, J. Therm. Anal. Calorim. **128**, 1007 (2017). doi 10.1007/s10973-016-6010-9
10. A. V. Ruseikina and O. V. Andreev, Russ. J. Inorg. Chem. **62**, 1134 (2017). doi 10.7868/S0044457X17020143
11. A. V. Ruseikina, L. A. Solov'ev, and O. V. Andreev, Russ. J. Inorg. Chem. **59**, 196 (2014). doi 10.1134/S0036023614030188
12. A. V. Ruseikina and L. A. Solov'ev, Russ. J. Inorg. Chem. **61**, 482 (2016). doi 10.1134/S0036023616040161
13. V. G. Bamburov and O. V. Andreev, Russ. J. Inorg. Chem. **47**, 598 (2002).
14. O. V. Andreev and A. V. Ruseikina, Russ. J. Inorg. Chem. **57**, 1502 (2012). doi 10.1134/S0036023612110034
15. N. V. Sikerina, O. V. Andreev, and I. P. Leven, Russ. J. Inorg. Chem. **53**, 455 (2008). doi 10.1007/s11502-008-3021-x
16. A. V. Ruseikina and Zh. A. Demchuk, Russ. J. Inorg. Chem. **62**, 27 (2017). 168 doi 10.1134/S0036023617010
17. N. V. Sikerina and O. V. Andreev, Russ. J. Inorg. Chem. **52**, 581 (2007). doi 10.1134/S0036023607040183
18. P. O. Andreev, E. I. Sal'nikova, and I. M. Kovenskii, Inorg. Mater. **50**, 1018 (2014). doi 10.1134/S002016851410
19. J. W. Visser, J. Appl. Crystallogr. **2**, 89 (1969).
20. M. F. Mansuetto, P. M. Keane, and J. A. Ibers, J. Solid State Chem. **101**, 1016 (1992). doi 10.1016/0022-4596(92)90182-U
21. L. A. Solovyov, J. Appl. Crystallogr. **37**, 743 (2004). doi 10.1107/S0021889804015638
22. K. Brandenburg, "Diamond," Visual Crystal Structure Information System Crustal Impact (Postfach, Boon).
23. N. B. Egorov and V. V. Shagalov, *Infrared Spectroscopy of Rare and Disseminated Elements: Educational and Methodological Guidelines for the Course "Physical and Chemical Methods of Analysis"* (Izd–vo TPU, Tomsk, 2008) [in Russian].
24. A. E. Christuk, P. Wu, and J. A. Ibers, J. Solid State Chem. **110**, 330 (1994).

Translated by V. Avdeeva